Neurobiology of Disease

MeCP2 in the Rostral Striatum Maintains Local Dopamine Content Critical for Psychomotor Control

San-Hua Su,[1] **Fang-Chi Kao,**[1] **Yi-Bo Huang,**[1] **and Wenlin Liao**[1,2]

[1]Institute of Neuroscience and [2]Research Center for Mind, Brain, and Learning, National Cheng-Chi University, Taipei 11605, Taiwan

Methyl-CpG binding protein 2 (MeCP2) is a chromatin regulator highly expressed in mature neurons. Mutations of *MECP2* gene cause >90% cases of Rett syndrome, a neurodevelopmental disorder featured by striking psychomotor dysfunction. In *Mecp2*-null mice, the motor deficits are associated with reduction of dopamine content in the striatum, the input nucleus of basal ganglia mostly composed of GABAergic neurons. Here we investigated the causal role of MeCP2 in modulation of striatal dopamine content and psychomotor function. We found that mice with selective removal of MeCP2 in forebrain GABAergic neurons, predominantly in the striatum, phenocopied *Mecp2*-null mice in dopamine deregulation and motor dysfunction. Selective expression of MeCP2 in the striatum preserved dopamine content and psychomotor function in both males and females. Notably, the dopamine deregulation was primarily confined to the rostral striatum, and focal deletion or reactivation of MeCP2 expression in the rostral striatum through adeno-associated virus effectively disrupted or restored dopamine content and locomotor activity, respectively. Together, these findings demonstrate that striatal MeCP2 maintains local dopamine content in a non-cell autonomous manner in the rostral striatum and that is critical for psychomotor control.

Key words: dopamine; methyl-CpG binding protein 2; motor control; Rett syndrome; striatum

Introduction

Rett Syndrome (RTT) is a neurodevelopmental disorder primarily affecting females. Numerous RTT patients develop stereotypical hand wringing with ambulatory difficulties; these motor symptoms usually exacerbate with age and resemble Parkinson's symptoms later in life (Chahrour and Zoghbi, 2007; Temudo et al., 2008). More than 90% of RTT cases are caused by mutations in the X-linked gene encoding methyl-CpG binding protein 2 (MeCP2; Amir et al., 1999). The MeCP2 protein is highly expressed in mature neurons and is involved in regulating target gene transcription (Chahrour and Zoghbi, 2007; Guy et al., 2011). Loss of MeCP2 in mice mimics many RTT-like symptoms including late onset hypoactivity and deficits in motor coordination and motor skill learning (Chen et al., 2001; Guy et al., 2001; Shahbazian et al., 2002; Goffin et al., 2012; Kao et al., 2015). These motor phenotypes have been previously linked to reduced dopamine synthesis in the midbrain dopaminergic neurons (Samaco et al., 2009; Gantz et al., 2011; Panayotis et al., 2011). However, MeCP2 deficiency in aminergic neurons does not show motor learning impairments (Samaco et al., 2009), and selective expres-

sion of MeCP2 in catecholamine neurons of *Mecp2*-deficient mice partially ameliorate the RTT-like motor deficits (Lang et al., 2013), raising the possibility that MeCP2 in noncatecholamine neurons also plays a role in psychomotor control.

We previously found that *Mecp2*-null mice show psychomotor deficits associated with aberrant molecular and cellular phenotypes in the striatum (Kao et al., 2015). The striatum is the input nucleus of the basal ganglia that resides in the forebrain and controls psychomotor behaviors. More than 98% of striatal neurons are GABAergic medium spiny neurons (MSNs), which integrate glutamatergic excitatory inputs from the cerebral cortex and dopaminergic afferents from the ventral midbrain. The MSNs project their axons to the substantia nigra (the striatonigral or direct pathway) or the globus pallidus (the striatopallidal or indirect pathway) to enhance or inhibit activities of the motor thalamus, respectively, and modulate execution of cortical motor commands (Kreitzer and Malenka, 2008). Previous studies have linked the disrupted corticostriatothalamic circuit or malfunctioned striatum to multiple neurological and psychiatric disorders presenting psychomotor symptoms, including autism and obsessive compulsive disorder (Crittenden and Graybiel, 2011; Peça et al., 2011). Moreover, mice lacking MeCP2 selectively in all GABAergic neurons, including those in the striatum, recapitulate most RTT-like phenotypes (Chao et al., 2010; Goffin et al., 2014), suggesting that MeCP2 in GABAergic neurons is engaged in pathogenesis of RTT. However, the functional role of MeCP2 in the striatum for psychomotor control remains unclear.

In this study, we took a genetic approach to selectively delete or preserve *Mecp2* expression predominantly in the striatum followed by characterization of motor phenotypes and dopamine content, as well as the expression of dopamine-related molecules

in the striatum. Together with an adeno-associated virus (AAV)-mediated viral approach to specifically alter *Mecp2* expression in selected regions of the striatum, we have dissected the anatomical origin of motor deficits in RTT-like mice.

Materials and Methods

Animals. Male *Mecp2* conditional knock-out (cKO; *Mecp2flox/y;Dlx5/6-Cre/+*) mice were generated by crossing male Dlx5/6-Cre transgenic mice [Cre; Tg(dlx6a-cre)1Mekk, Jackson Laboratories; Monory et al., 2006] with heterozygous Floxed-*Mecp2* [Flox; *Mecp2Jaenisch.Flox/+*, Mutant Mouse Regional Resource Center (MMRRC) at UC Davis] female mice in which the exon 3 of *Mecp2* gene was flanked by the *loxP* sites (Chen et al., 2001). The experimental cohorts of *Mecp2* conditional rescue (cRes; *Mecp2stop/y;Dlx5/6-Cre/+*) mice were generated by crossing the same Cre males with heterozygous floxed-STOP-*Mecp2* (STOP; *Mecp2stop/+*, Jackson Laboratories) female mice, which were established by insertion of *loxP*-flanked-STOP-Neo cassette into intron 2 of *Mecp2* gene (Guy et al., 2007). Four- to 5-week-old male cKO or cRes mice were used. To study the rescue effects in females, 4- to 5-week-old and 8- to 10-week-old female cRes mice were also used. In addition, Flox and STOP mice at 4–5 weeks of age were used for AAV experiments. All mice used in this study have been backcrossed to C57BL/6 mice (National Laboratory Animal Center, Taiwan) for at least 10 generations and maintained in C57BL/6 background. All mice were housed in individually ventilated cages (Alternative Design) at $22 \pm 2°C$ with $60 \pm 10\%$ humidity under a 12 h light/dark cycle (light on 08:00–20:00). Irradiated diet and sterile water were available *ad libitum*. All experiments were approved by the Institutional Animal Care and Use Committee at National Cheng-Chi University.

Genotyping. Mice were weaned and ear-tagged at postnatal days 21–23, and then genotyped as previously described (Kao et al., 2015). Briefly, the tail tissues of mice were lysed with protease K (100 μg/ml, Amresco) at 55 °C for overnight and genomic DNA was extracted by protein precipitation solution (Promega). One microliter of genomic DNA was used for genotyping by PCR. The sequence of primers for genotyping of Cre, STOP, and Flox mice was obtained from the Jackson Laboratory or MMRRC. The PCR products of a 320 bp fragment was identified as Cre-positive genotype. For Flox mice, PCR products of 280 and 180 bp were identified as Flox and WT allele, respectively. For genotyping of STOP mice, the bands of 379 and 222 bp were identified as WT and STOP allele, respectively.

Stereotaxic surgery for AAV injection. Male Flox or STOP mice and their littermate WT controls at the age of 4–5 weeks were used for AAV study as previously described (Adachi et al., 2009). Briefly, mice were anesthetized with 5% isoflurane (diluted with oxygen) before be mounted on a stereotaxic apparatus (David Kopf Instruments), and maintained sleeping with 1% isoflurane during surgery. The coordinates of target injection sites relative to bregma were AP +1.5 mm, ML ±1.5 mm, DV −3.5 mm for the rostral striatum (ST-r); and AP +0.1 mm, ML ±2.2 mm, DV −4.0 mm for the caudal striatum (ST-c). Through a Hamilton syringe with a 30 gauge needle, 1 μl of AAV vector (9.63×10^{11} genome copy/μl) was bilaterally delivered into the target regions in 5 min and the needle was left in place for 5 min postinjection to ensure diffusion of the vector. All mice were injected either with saline or AAV-Cre-GFP (AAV2/9.CMV.HI.eGFP-Cre.WPRE.SV40, PV2004, Vector Core at University of Pennsylvania), which expresses the Cre recombinase fused with eGFP. After surgery, mice were continuously monitored for general health and subjected to open-field test at postinjection days 7, 14, and 21. One set of the AAV-injected brains (n = 4–7) was harvested at postinjection day 14 for dopamine content measurement with high-performance liquid chromatography (HPLC); another set of brains (n = 3) was perfused for immunofluorescence examination of GFP and MeCP2 expression. The "transduction efficiency" was estimated as percentage of GFP-positive area in total striatal area on the two sections with the highest transduction rate (see Fig. 5C). The transduction efficiency was also estimated by measuring the proportion of GFP-positive cells in total cells labeled with 4′,6-diamidino-2-phenylindole (DAPI) in a region of 200×200 μm around the needle tip (see Fig. 5D). The "recom-

bination efficiency" was estimated as the percentage of MeCP2-negative cells in total GFP-positive cells in the region of 200×200 μm around the needle tip (see Fig. 5G).

Preparation of brain tissues. After behavioral testing, a group of the mice (n = 4–8 for each genotype) were sacrificed by cervical dislocation. Tissues from the striatum (ST-r, ST-m, ST-c) and the cerebral cortex (CTX-r, CTX-m, CTX-c) were microdissected on ice at the position of bregma +1.54 mm (rostral), +0.86 mm (middle), and +0.14 mm (caudal) with the aid of brain slicer matrix (Zivic Instrument) and punches (diameter: 1.5 mm for ST-r, CTX-r, CTX-m, and CTX-c; 1.75 mm for ST-m; 2.0 mm for ST-c; Ted Pella; see Fig. 2A). Tissues of the ventral midbrain (VMB; at bregma −3.28 mm) were collected manually from the same animals according to the atlas (Paxinos and Franklin, 2004). The tissues were frozen in liquid nitrogen immediately after dissection and then kept at −80°C until further analysis by HPLC or Western blotting. Another set of animals (n = 4–6 per group) were anesthetized by isoflurane and perfused with 4% paraformaldehyde (Sigma-Aldrich) in PBS (Liao et al., 2005). The brains were postfixed for at least 16 h in the same fixatives, cryo-protected in 30% sucrose (Merck) in PBS for 36–48 h, and embedded in OCT compound (Tissue-Tek, Sakura Finetek) before sectioning by cryostat (CM3050S, Leica). The brain sections were stored in PB buffer with 0.1% sodium azide (Sigma-Aldrich) for immunohistochemical analysis with the indicated antibodies (see below).

Dopamine measurement by HPLC. The dopamine content of different brain regions in mice was measured by HPLC with an electrochemical detection system as described previously (Kao et al., 2015). Briefly, brain tissues were homogenized on ice with perchloric acid containing 0.45 mM sodium hydrosulfite immediately before measurement. After sonication, the lysate was centrifuged at $15,000 \times g$ for 10 min at 4°C and filtered through syringe with 0.22 μm nylon filters (Millipore). Twenty microliters of sample lysate was injected through auto-sampler. The mobile phase (100 mM $NaH_2PO_4 \cdot H_2O$, 0.74 mM heptane-1-sulfonic acid sodium salt, 0.027 mM EDTA, 2 mM KCl, and 10% methanol; adjusted to pH 3 with phosphoric acid) was filtered and degased for 30 min, and then pumped into the separation system of a C18 column (250×4.6 mm, Grace Alltima) through an electrochemical flow cell (Antec) at a flow rate of 0.8 ml/min. The pure compounds of dopamine, 3,4-dihydroxyphenylacetic acid and homovanillic acid (Sigma-Aldrich) were dissolved in lysis buffer at the concentration of 20, 100, and 500 ng/ml and served as standard controls. For comparison of dopamine content, the integrated areas of the dopamine peaks in cKO mice were quantified by DataApex software (Clarity) and normalized with the ones in Flox control mice.

Western blot analysis. Brain tissues were homogenized by sonication in lysis buffer containing 1% protease inhibitors and phosphatase inhibitors (Sigma-Aldrich). Twenty micrograms of protein was separated by PAGE (10%, Bio-Rad) with 60 V for 30 min and 120 V for 1.5 h and then transferred to a PVDF membrane (Millipore) by liquid electroblotting (Mini Trans-Blot Cell, Bio-Rad) with 350 mA for 1 h. The membrane was blocked by skim milk and incubated with primary antibodies against MeCP2 (1:2000; Zhou et al., 2006), dopamine D2 receptor (DRD2, 1:1000, Millipore), tyrosine hydroxylase (TH; 1:20,000, Millipore), phosphor-TH at Ser40 (pTH-Ser40, 1:2000, Symansis), or glyceraldehyde 3-phosphate dehydrogenase (GAPDH; 1:100,000, Millipore) at 4°C for 16 h. Following incubation with peroxidase-conjugated goat-anti-rabbit or goat-anti-mouse secondary antibodies (1:100,000) at room temperature for 2 h, the expression of the interested proteins was detected by an enhanced chemoluminescence reagent kit (Millipore) under a bioimage acquisition system (Xlite 200R, Avegene Life Science). To measure the levels of phosphorylated TH and total TH proteins, we first probed the blot with an antibody against pTH-Ser40. The blot was then stripped using a Western blot stripping buffer (Millipore). Upon confirming no leftover signal, the same blot was probed again with an antibody against total TH. The intensity of target protein expression was normalized with that of GAPDH by densitometry-based quantification with ImageJ (NIH). The expression levels of interested proteins were presented as "percentage of Flox."

Immunohistochemistry. Immunostaining was performed as described previously (Liao et al., 2008). Briefly, free-floating brain sections of 20

μm were pretreated with 0.1 M PBS containing 0.2% Triton X-100, 3% H₂O₂, and 10% methanol for 10 min, and then blocked with 3% normal goat serum in 0.1 M PBS. Sections were incubated with the rabbit poly-clonal primary antibodies against MeCP2 (1:2000; Zhou et al., 2006) at room temperature for 16 h, followed by incubation with biotinylated goat-anti-rabbit secondary antibody (1:500, Vector Laboratories) in 0.1 M PBS containing 1% normal goat serum at room temperature for 2 h. Sections were then incubated for 1.5 h with avidin-biotin-complex (Elite ABC kit, Vector Laboratories) and immunoreactivities were detected with 0.02% diaminobenzidine (DAB; Sigma-Aldrich) in the presence of 0.0002% H₂O₂ (Sigma-Aldrich) and 0.08% nickel ammoniosulfate (Sigma-Aldrich). Brain sections from cKO or cRes mice were processed in parallel with the sections from their littermate control mice, and color-developed in DAB solution for exactly the same duration as control sections. For immunofluorescence staining, the primary antibody-treated sections were incubated with the goat-anti-rabbit secondary antibodies conjugated with AlexaFluor-488 or Alexa Fluor-555 (Invitrogen) for 2 h, followed by counterstaining with DAPI. Photomicrographs were taken by an upright microscopic system (Imager D2, Zeiss) equipped with a CCD camera (ORCA-R2 C10600−10B, Hamamatsu).

Behavioral assays. All the behavioral assays were performed in a sound-reduced room during 12:00–6:00 P.M. on the testing day by unbiased operators blinded to genotypes.

Open-field activity. Mutant mice and their littermate controls at 4–5 weeks of age were tested as described previously (Kao et al., 2015). The mice were videotaped within a clear Plexiglas open-field arena (40 × 40 × 25 cm) for 16 min under dim light. Parameters of locomotor activity, including total distance traveled, percentage of resting time, average and maximal locomotion velocity, and percentage of time spent in the central arena were analyzed for the last 12 min (from 3.5 to 15.5 min, excluding the first 3.5 min of habituation period) with the Smart video-tracking system (Harvard). Body movements at speeds under the detection threshold for locomotion (2 cm/s) were counted as resting. The activity of mutant mice was normalized with the average activity of control mice (shown as percentage of WT). Differences between genotypes were analyzed by one-way ANOVA.

Accelerating rotarod task. Mice were tested for motor coordination and motor skill learning as described previously (Cox et al., 2009). Briefly, mice were trained for 30 s at a constant speed of 4 rpm on the rotarod apparatus (LE8200, PanLab). Thirty minutes after training, mice were tested on the rotarod at an accelerating speed (4–40 rpm within 5 min). Three testing trials were performed on each day for 5 consecutive days with an intertrial interval of 30 min. The latency of a mouse falling off the rotating rod was recorded automatically by the stop-plates. The median of three trials on each test day was adopted for statistical analysis by repeated-measures two-way ANOVA followed by Bonferroni *post hoc* test.

Barnes maze. Mice were tested by the Barnes maze to examine spatial learning and memory as described previously (Barnes, 1979). The testing apparatus is an elevated (50 cm above the floor) circular Plexiglas plate (92 cm diameter) with 20 holes (5 cm diameter, 7.5 cm between holes) evenly spaced around the perimeter. Mice were trained on the plate to identify an escape box (21 × 10 × 7 cm) hidden behind the target hole, which was designated as an analog to the hidden platform in the Morris water maze task. The location of the target hole was selected for a given mouse but randomized across mice. Mice were initially placed in the center of the plate covered by an opaque cylinder, and the cylinder was removed 10 s after the beginning of the trial with an aversive tone (440 Hz, 76 dB) switched on. Mice were trained to locate the target hole according to surrounding visual cues and escape from the aversive tone for three training trials per day over 3 consecutive days. The spatial memory was measured by the "probe test" performed on the second day and 7 d after the last training trial. All the training trials and the probe trials were videotaped for 3 min, and then the escape latency for the training trials and the percentage of time in different quadrants (target, left, right, and opposite) during the probe test were analyzed. The performance of mutants and controls was compared by repeated-measures two-way ANOVA.

Elevated zero maze. The anxiety state of mice was measured with an elevated zero maze as described previously (Shepherd et al., 1994). The apparatus consists of a circular platform (6.1 cm width, 45 cm inner diameter) that is equally divided into four quadrants. Two quadrants on opposite sides of the platform are enclosed by walls (15 cm high); the other two quadrants are opened and bordered by a lip (0.6 cm high). The maze was set 50 cm above the floor and an overhead camera was set to videotape mouse activity. Each mouse was tested on the maze for 5 min and the time it spent in the opened quadrants was quantified and analyzed.

Statistics. All results were reported as mean ± SEM, and the groups were compared using Student's *t* test, one-way ANOVA or repeated-measures two-way ANOVA followed by Bonferroni *post hoc* test using Prism 5 (GraphPad), as specifically noted in the figure legends.

Results

Loss of striatal MeCP2 impairs psychomotor function

To address the causal role of striatal MeCP2 in psychomotor control, we generated mice lacking MeCP2 predominantly in the striatum by crossing floxed-*Mecp2* (Chen et al., 2001) females to Dlx5/6-Cre (Monory et al., 2006) males. The Dlx5/6-Cre mice express Cre recombinase in forebrain GABAergic neurons and have been used in numerous studies conducting selective dele-tion of striatum-enriched genes (Ohtsuka et al., 2008; Shen et al., 2008; Yu et al., 2009; Zhao et al., 2013). Immunostaining showed that MeCP2 expression is abolished in the striatum (ST) while maintained in the primary motor cortex (M1), amygdala (Amyg), and cerebellum (Cbll) of *Mecp2* ^flox/y;^*Dlx5/6-Cre/+* (cKO) mice compared with the littermate floxed-*Mecp2* mice (*Mecp2* ^flox/y^; Flox; Fig. 1A–D).

Given that *Mecp2* is an X-linked gene, we began our studies on male mice to avoid the confounding effects of mosaic MeCP2 expression in females. The cKO mice and their littermate con-trols, including *Mecp2*^+/y^ and *Mecp2*^+/y^;*Dlx5/6-Cre/+* (WT and Cre, respectively), as well as Flox mice at 4–5 weeks of age were then subjected to an open-field test. We found that cKO mice traveled significantly shorter distances (73.0 ± 3.8% of WT, $p <$ 0.001) at reduced average velocity (80.8 ± 2.4% of WT, $p <$ 0.001) and maximal velocity (76.8 ± 3.2% of WT, $p < 0.001$) with increased immobile time (121.8 ± 5.3% of WT, $p < 0.01$), indicated that cKO mice were less active than controls (Fig. 1E). No significant difference was found among the WT, Cre, and Flox control groups in any of the measured parameters. In addition, we found that cKO mice did not exhibit thigmotaxis in open-field test (Fig. 1E) and spent similar amount of time in the opened quadrants as control mice when tested in an elevated zero maze (Fig. 1H). This is in contrast to increased anxiety observed in *Mecp2*-null mice (Kao et al., 2015), suggesting that the hypoac-tivity shown in cKO mice is not caused by increased anxiety.

The same cohorts of mice were next tested on an accelerated rotarod for 5 consecutive days to assess motor coordination and motor skill learning. We found that cKO mice showed compara-ble falling latency to controls on the first two testing days, indi-cating a normal motor coordination in the initial stage (Fig. 1F). By comparing the performance of each genotype across all 5 test-ing days, we found that cKO mice showed significant difference from the control mice ($F_{(3,26)} = 7.506, p = 0.0009$) and failed to acquire motor skills from day 3 to day 5 ($p > 0.05$ compared with Day 1). On the final testing day, cKO mice stayed significantly shorter time on the rotarod than WT mice ($p = 0.0063$). To-gether, these results suggest that loss of MeCP2 predominantly in the striatum reduces locomotor activity and impairs motor skill learning, consistent with most of the motor deficits observed in *Mecp2*-null mice (Kao et al., 2015).

In contrast to deficits in motor skill learning, cKO mice showed similar escape latency to their littermate controls when
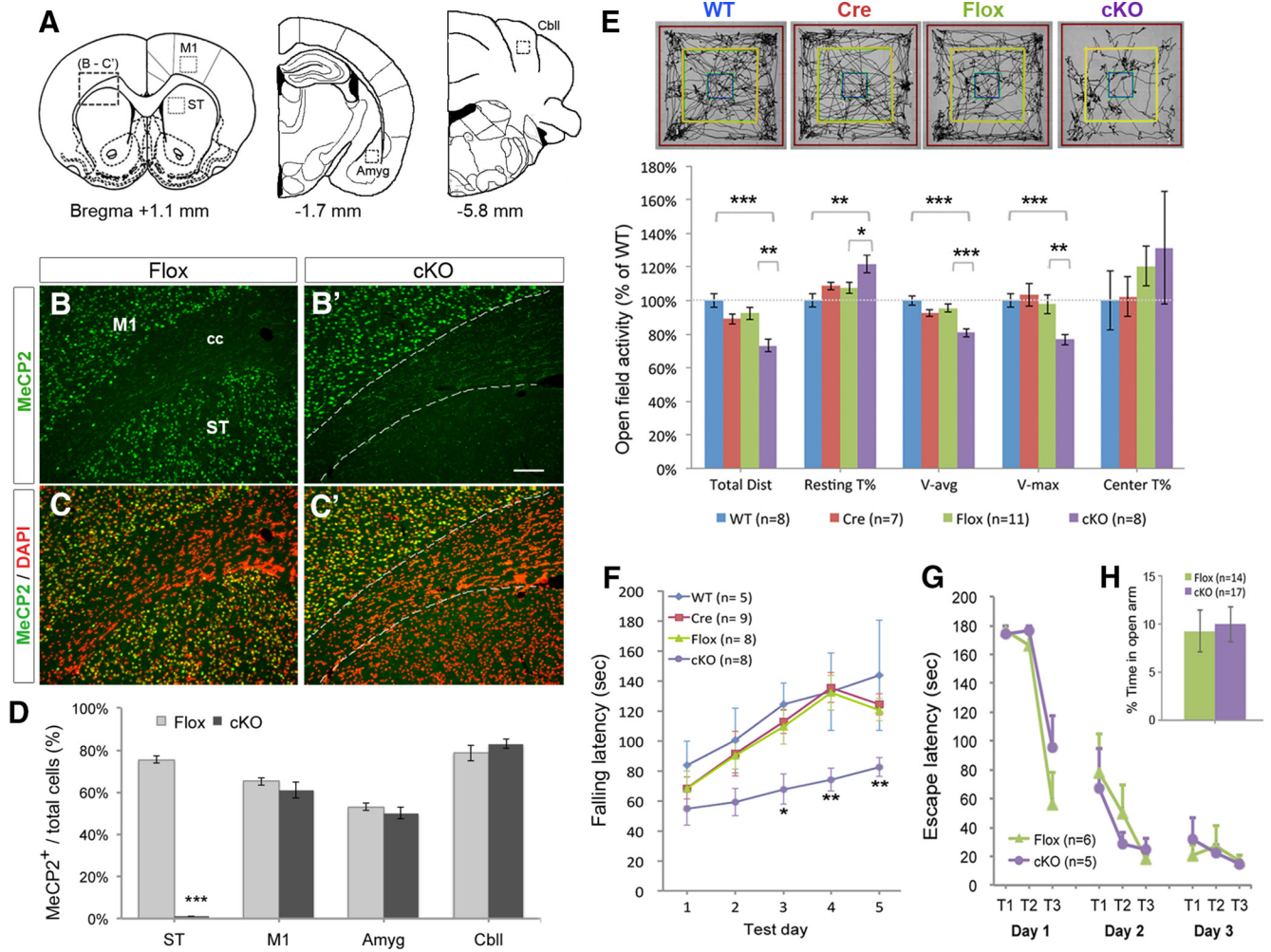
Figure 1. Loss of striatal MeCP2 impairs psychomotor behaviors. ***A***, Schematic diagrams illustrate the selected brain regions for immunostaining and quantification of MeCP2-positive cells in ***B–D***. The area of squares is 200 × 200 μm. ***B–D***, Selective reduction of MeCP2-expressing cells in the striatum of cKO mice compared with Flox controls. Total cells are labeled by DAPI (pseudo-colored in red). cc, corpus callosum. Scale bar (in ***B′***), 100 μm. ***E***, Reduced locomotor activity of cKO mice in open-field test. The representative exploration trajectories are shown in the top panel. Total Dist., Total distance traveled; Resting T%, percentage of time at rest; V-avg, average velocity of locomotion; V-max, maximal velocity of locomotion; Center T%, percentage of time stayed in the central arena (yellow square). ***F***, Impaired motor skill learning in cKO mice tested by accelerating rotarod. ***G***, No spatial learning deficit in cKO mice tested by Barnes maze. T1, Trial 1. ***H***, Unaltered anxiety state in cKO mice tested by elevated zero maze; $*p < 0.05$, $**p < 0.01$, $***p < 0.001$, compared with controls by Student's t test in ***D*** ($n = 4$) and ***H***, one-way ANOVA in ***E***, repeated-measures two-way ANOVA in ***F*** and ***G***, followed by Bonferroni *post hoc* test (***F***).

tested in Barnes maze (Fig. 1G), suggesting that MeCP2 in forebrain GABAergic neurons is essential for motor skill leaning but dispensable for spatial learning, at least at 1 month of age. In addition, we observed that most cKO male mice older than 5 months of age developed behavioral seizures upon handling (e.g., as lifting the wire top of the cage). The seizure phenotype was barely found in cKO mice younger than 3 months, suggesting that the motor deficits found in mice at 4–5 weeks old are unlikely the consequences of seizures. Notably, similar seizure phenotype was observed in previous studies using the same Cre and floxed *Mecp2* mouse lines (Goffin et al., 2014), but not in cKO mice generated using a different floxed *Mecp2* mouse line (Chao et al., 2010). This is likely due to the different floxed allele of *Mecp2* and different genetic background.

Loss of striatal MeCP2 disrupts dopamine synthesis in the striatum

We previously found a rostral-to-caudal gradient of dopamine reduction in the striatum of *Mecp2*-null mice (Kao et al., 2015), raising the possibility that MeCP2 modulates striatal dopamine content in a subregion-specific manner. To measure dopamine content in cKO mice, we harvested brain tissues from different striatal regions and the VMB, where the dopaminergic neurons are located (Fig. 2A). We found that the amount of dopamine was significantly reduced in the rostral striatum (ST-r, 48.7 ± 8.3%, $p < 0.001$), increased in the caudal striatum (ST-c, 140.5 ± 18.1%, $p < 0.05$), but not altered in the middle striatum (ST-m, 99.6 ± 13.7%, $p > 0.05$) and VMB (106.8 ± 6.0%, $p > 0.05$) of cKO mice compared with littermate Flox controls ($n = 6$; Fig. 2B,C).

To examine the cause of aberrant dopamine content in the striatum of cKO mice, we next measured protein expression of the rate-limiting enzyme for dopamine synthesis, TH and its active form, phosphorylated TH at serine 40 (pTH-Ser40; Funakoshi et al., 1991). We found that the total amount of TH protein remained unchanged in the ST-r (90.6 ± 14.3%, $p > 0.05$), but the phosphorylation of TH (pTH-Ser40), an indicator of TH activity, was significantly reduced (65.8 ± 9.2%, $p < 0.01$, $n = 4$; Fig. 2D,E). In addition, both the total protein of TH and pTH-Ser40 was increased in the ST-c (TH: 140.9 ± 5.7%, $p < 0.001$;
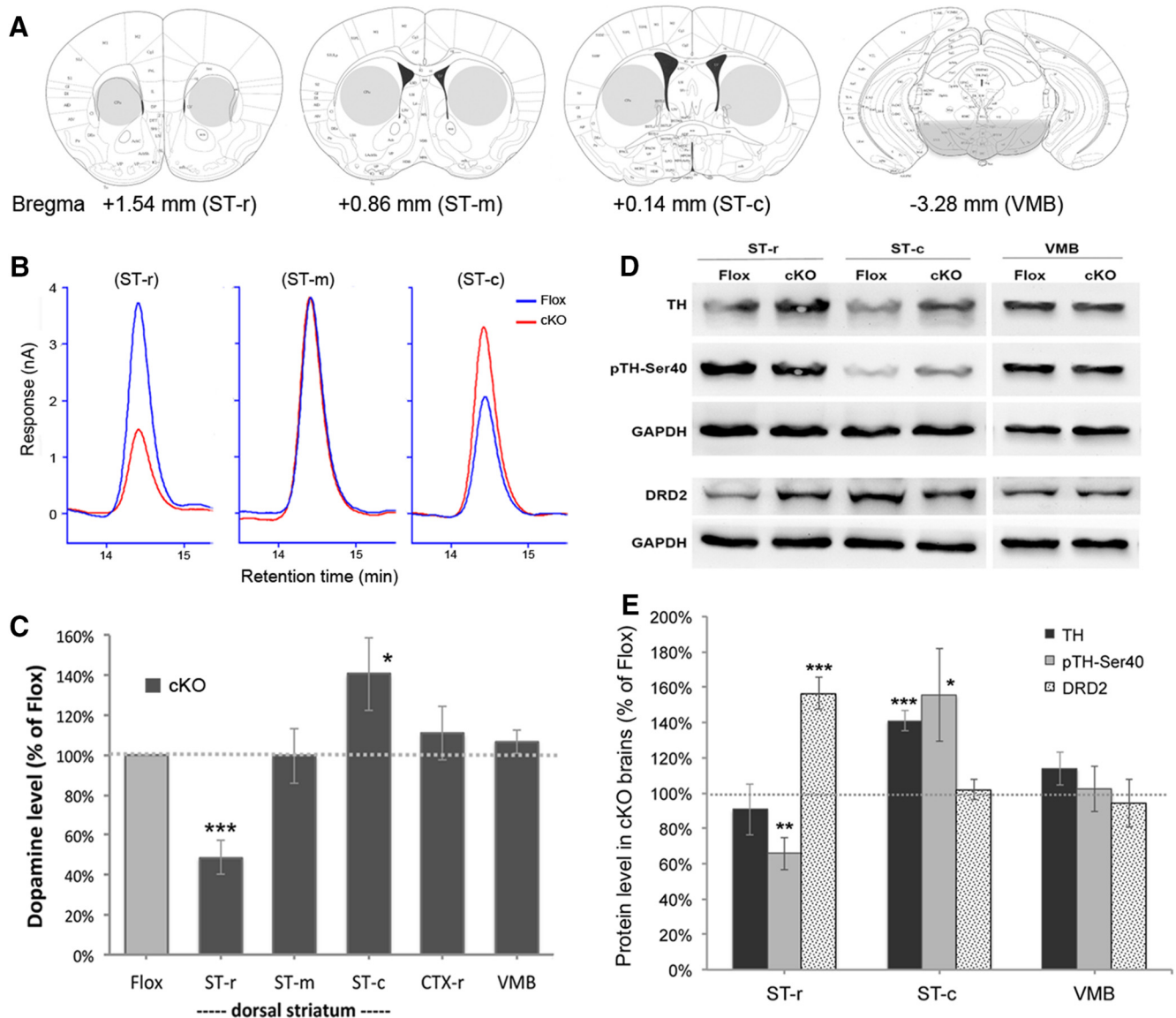
Figure 2. Non-cell autonomous alterations of dopamine synthesis in the striatum of cKO mice. *A*, Anatomical illustrations showing the selected brain regions (gray area) harvested for analysis. *B*, *C*, HPLC measurement shows reduction of dopamine content in the ST-r, but increase in the ST-c of cKO mice. Note that the dopamine content in the VMB (*C*) was unchanged. *D*, *E*, Immunoblotting shows the expression of TH, pTH-Ser40, and DRD2 in the selected brain regions of cKO mice and the littermate Flox controls. GAPDH, the internal control; *p < 0.05, **p < 0.01, ***p < 0.001, compared with Flox controls by Student's *t* test (n = 4 – 6).

pTH: 155.5 ± 26.2%, $p < 0.05$; $n = 4$) of cKO mice. No difference was found in levels of total TH or pTH-Ser40 in the VMB of cKO mice compared with littermate Flox controls (Fig. 2*D*,*E*). The consistent reduction of pTH-Ser40 level and dopamine content in the ST-r and consistent increase of total TH and dopamine content in the ST-c without alterations in the VMB, suggest that loss of striatal MeCP2 disrupts local dopamine synthesis non-cell autonomously in selective subregion of the striatum.

Given that the TH phosphorylation is inhibited by activation of DRD2 (Lindgren et al., 2001), we also examined DRD2 protein expression in the striatum of cKO mice. Immunoblotting results showed that DRD2 was significantly increased in the ST-r (156.4 ± 8.9%, $p < 0.001$), but unchanged in the ST-c (102.0 ± 5.8%, $p > 0.05$) and VMB (94.1 ± 13.5%, $p > 0.05$) of cKO mice compared with Flox controls ($n = 5$; Fig. 2*D*,*E*), consistent with previous findings in *Mecp2*-null mice (Kao et al., 2015). Therefore, selective removal of MeCP2 from the striatum likely reduces

dopamine synthesis in the ST-r by increasing local expression of DRD2 that suppresses TH activity.

MeCP2 in the striatum preserves striatal dopamine and psychomotor function

To examine whether selective expression of MeCP2 in the striatum is sufficient to preserve striatal dopamine content and psychomotor function, we crossed floxed-STOP-*Mecp2* females (*Mecp2*$^{stop/+}$; STOP mice; Guy et al., 2007) to the Dlx5/6-Cre males (Monory et al., 2006). We found that MeCP2 was barely detected in male STOP mice (*Mecp2*$^{stop/y}$; Fig. 3*A′*–*C′*,*D*), similar to those observed in *Mecp2*-null mice (Guy et al., 2007). With expression of Cre recombinase in forebrain GABAergic neurons, *Mecp2*$^{stop/y}$;*Dlx5/6-Cre/+* mice (cRes mice) preserved MeCP2 expression to the WT level selectively in the striatum (Fig. 3*A″*,*D*). MeCP2 protein was also detected in sparse neurons at the primary motor cortex (M1; Fig. 3*B″*,*D*), but the number of MeCP2^{+}
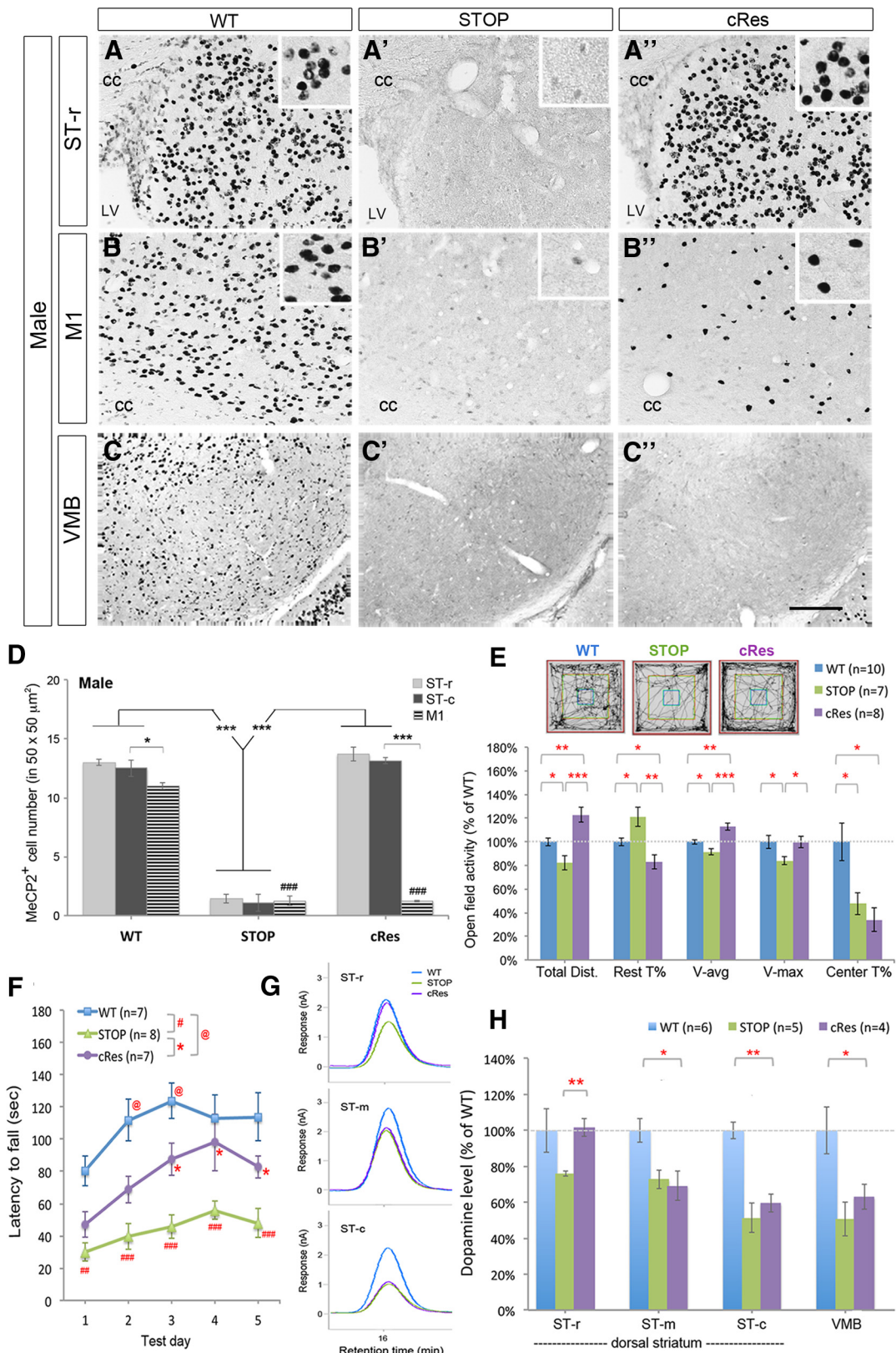
Figure 3. Expression of striatal MeCP2 preserves psychomotor function and dopamine content in the rostral striatum. ***A–D***, Selective preservation of MeCP2 in the striatum of cRes mice. MeCP2 was barely detected in STOP mice (***A′–C′***). Insets in ***A–B″*** show high-magnification images of MeCP2-positive nuclei in a square of $50 \times 50 \ \mu m^2$. Scale bar (in ***C″***), 100 μm. cc, Corpus callosum; LV, lateral ventricle. $n = 3$ for each group in ***D***. ***E***, Preservation of locomotor activity in cRes mice tested in an open field. ***F***, Restoration of motor skill learning in cRes mice on the acceleration rotarod test. ***G–H***, Expression of striatal MeCP2 preserves dopamine content selectively in the ST-r of cRes mice. Data are shown as mean ± SEM;*,@$p < 0.05$; **, ##$p < 0.01$; ***, ###$p < 0.001$; compared with control mice (as indicated) by one-way ANOVA in ***D***, ***E***, and ***H***; repeated measured two-way AVOVA in ***F***, followed by Bonferroni *post hoc* test. ### in ***D***, comparing M1 of STOP or cRes to that of WT.

cells in the M1 of cRes mice was not significantly restored compared with STOP and WT controls (Fig. 3D). No MeCP2 expression was restored in the VMB of cRes mice (Fig. 3C″). These results reflected the regional specificity of Cre-dependent restoration of MeCP2 expression in cRes mice.

Similar to the hypoactivity observed in *Mecp2*-null mice, STOP mice traveled shorter distance (82.0 ± 5.9% of WT, $p <$ 0.05), took more resting time (121.2 ± 8.1% of WT, $p <$ 0.05), and moved with lower average velocity (91.5 ± 2.7% of WT, $p <$ 0.05) and lower maximal velocity (84.0 ± 3.5% of WT, $p <$ 0.05) in open-field test compared with WT controls (Fig. 3E). With MeCP2 expression in the striatum, cRes males traveled longer distance than controls (122.9 ± 6.2% of WT, genotype effect: $F_{(3,36)} = 16.98$, $p < 0.0001$, one-way ANOVA), showing "overshoot" locomotor activity compared with WT mice (Fig. 3E). The cRes mice also took less time for rest and traveled in higher average velocity and maximal velocity compared with STOP mice (Fig. 3E). The anxiety-like behavior in STOP mice, shown as reduced time spent in the central arena, was remained in cRes mice (34.0 ± 9.8% of WT, $p > 0.05$ compared with STOP mice).

By testing on an accelerating rotarod, STOP and cRes mice showed remarkable difference in motor coordination and motor skill learning over 5 testing days compared with WT mice ($F_{(2,19)} =$ 17.04, $p < 0.0001$). An increased falling latency was observed in cRes mice from testing day 3 to day 5 ($p < 0.05$ compared with STOP mice; Fig. 3F). Notably, the motor skill learning in cRes mice was restored to WT level on testing Days 4 and 5 ($p > 0.05$ compared with WT mice; Fig. 3F). Therefore, expression of MeCP2 in the striatum sufficiently improves psychomotor deficits in MeCP2-deficient mice.

Moreover, preservation of motor function in cRes mice was accompanied with restored dopamine content specifically in the ST-r (76.0 ± 1.3% of WT in STOP vs 101.7 ± 5.1% of WT in cRes; $p < 0.01$). The preservation of dopamine was not found in the ST-m, ST-c and VMB of cRes mice compared with WT controls (Fig. 3G,H). Together, these results suggest that preserved expression of MeCP2 selectively in the striatum is sufficient to maintain dopamine content in the striatum, particularly in the ST-r, and ultimately contributes to the restoration of psychomotor behaviors.

Preservation of psychomotor function and dopamine content in female mice

Given that RTT primarily affects females, we next examined the effects of preserving striatal MeCP2 expression in heterozygous female cRes mice. Consistent with previous findings, MeCP2 exhibited a mosaic expression in female STOP mice (Fig. 4A′; Guy et al., 2007). In contrast, MeCP2 expression was preserved to WT level selectively in the striatum, but not in the M1 of cRes females (Fig. 4A–C). We noticed that STOP female mice at 4–5 weeks of age began to exhibit impaired locomotion and motor skill learning compared with WT controls, however, these psychomotor deficits were restored to control level in cRes females (Fig. 4D,E). Importantly, the motor skill learning of cRes females was further improved when they were tested again on the rotarod at 8–10 weeks of age, in contrast to that in STOP female mice (Fig. 4F).

When we measured the dopamine content, we found a significant reduction of dopamine levels in both the ST-r and ST-c of STOP females (Fig. 4G). However, the dopamine content was preserved to nearly WT level in cRes mice at the ST-r (46.8 ± 3.7% of WT in STOP vs 85.2 ± 5.4% of WT in cRes, $p < 0.001$) but not at the ST-c (53.3 ± 7.4% of WT in STOP vs 58.5 ± 9.4% of WT in cRes, $p > 0.05$; Fig. 4G). The preserved dopamine

content in the ST-r was unlikely resulted from dopaminergic inputs from the midbrain, as the dopamine level in the VMB of cRes mice was not restored (Fig. 4G). Thus, selective preservation of MeCP2 expression in the striatum of heterozygous female mice is sufficient to ameliorate RTT-like motor deficits and preserve dopamine content in the ST-r, providing the clinical relevance of this study to female patients of RTT.

Mecp2 in the rostral striatum controls dopamine content and locomotion

To specifically address the role of MeCP2 in selective locations of the striatum and exclude any confounding effects of Dlx5/6-Cre-mediated recombination in brain regions other than the striatum, we next performed a virus-mediated focal deletion of *Mecp2* in the ST-r or ST-c. By stereotaxic injection of AAV vector expressing a Cre recombinase/green fluorescent protein (Cre-GFP) fusion protein in the ST-r (Fig. 5A) or ST-c, (Fig. 5B), we found that the estimated striatal volume expressing GFP in the ST-r was ∼25–30% (26.9 ± 1.3% in WT, 30.4 ± 1.9% in Flox, $n = 3$; Fig. 5A,C). Approximately 85–90% of DAPI-positive striatal cells around the injection site are GFP-positive (88.9 ± 3.4% in WT, 86.6 ± 4.9% in Flox, $n = 3$; Fig. 5D). Almost all GFP-positive cells are MeCP2-negative in Flox mice (98.4 ± 0.4%, $n = 3$; Fig. 5F–F′, green arrowheads) but most of GFP-positive cells maintained MeCP2 expression in WT mice (Fig. 5E–E′, green arrowheads), suggesting efficient ablation of MeCP2 expression using this approach. These results indicate that injection of AAV-Cre-GFP allowed manipulation of MeCP2 expression selectively in the ST-r or ST-c by highly efficient Cre-mediated recombination (Fig. 5G).

After surgery, we subjected the mice to an open-field test every 7 d for 3 weeks. To set the baseline, these mice were also tested on the day before AAV injection. We found that all Flox and WT mice traveled similar distances before AAV-injection (Day 0; Fig. 6A). In contrast, the AAV-injected Flox mice traveled significantly shorter distances on day 14 after surgery (80.9 ± 2.5% of Day 0, $p < 0.001$; Fig. 6B) with reduced average speed compared with AAV-injected WT mice. Notably, focal deletion of *Mecp2* in the ST-c of Flox mice did not impair their locomotor activity (Fig. 6D,E), suggesting that MeCP2 in the ST-r is required for mobility control.

We next examined the dopamine content from different subregions of the striatum and midbrain harvested at 14 d after AAV-injection. Mice with *Mecp2* deletion in the ST-r showed reduced dopamine content specifically in the ST-r (61.5 ± 3.4% of WT, $p < 0.001$) but no change in the ST-m and ST-c (Fig. 6C). By contrast, injection of AAV-Cre to the ST-c reduced dopamine content locally in the ST-c (62.7 ± 5.2% of WT, $p < 0.01$) but not in the ST-r or ST-m (Fig. 6F). Notably, deletion of *Mecp2* in either ST-r or ST-c did not alter dopamine content in the VMB (Fig. 6C,F). Thus, MeCP2 expression in specific regions of the striatum is necessary to maintain local dopamine content.

To further examine whether MeCP2 expression in the ST-r is sufficient to restore locomotion, we next reactivated MeCP2 expression in the ST-r of STOP mice. We found that the STOP mice exhibited a trend of hypoactivity before AAV injection (Day 0; Fig. 6G), likely reflecting the beginning of symptomatic onset at this age (4–5 weeks of age). The STOP mice gradually developed significant hypoactivity compared with WT littermates at ∼6 weeks of age (71.6 ± 8.6% of WT, $p = 0.05$; Fig. 6H). Upon delivering AAV into the ST-r for 14 d, the STOP mice showed significantly rescued locomotor activity (149.9 ± 9.1% of WT,
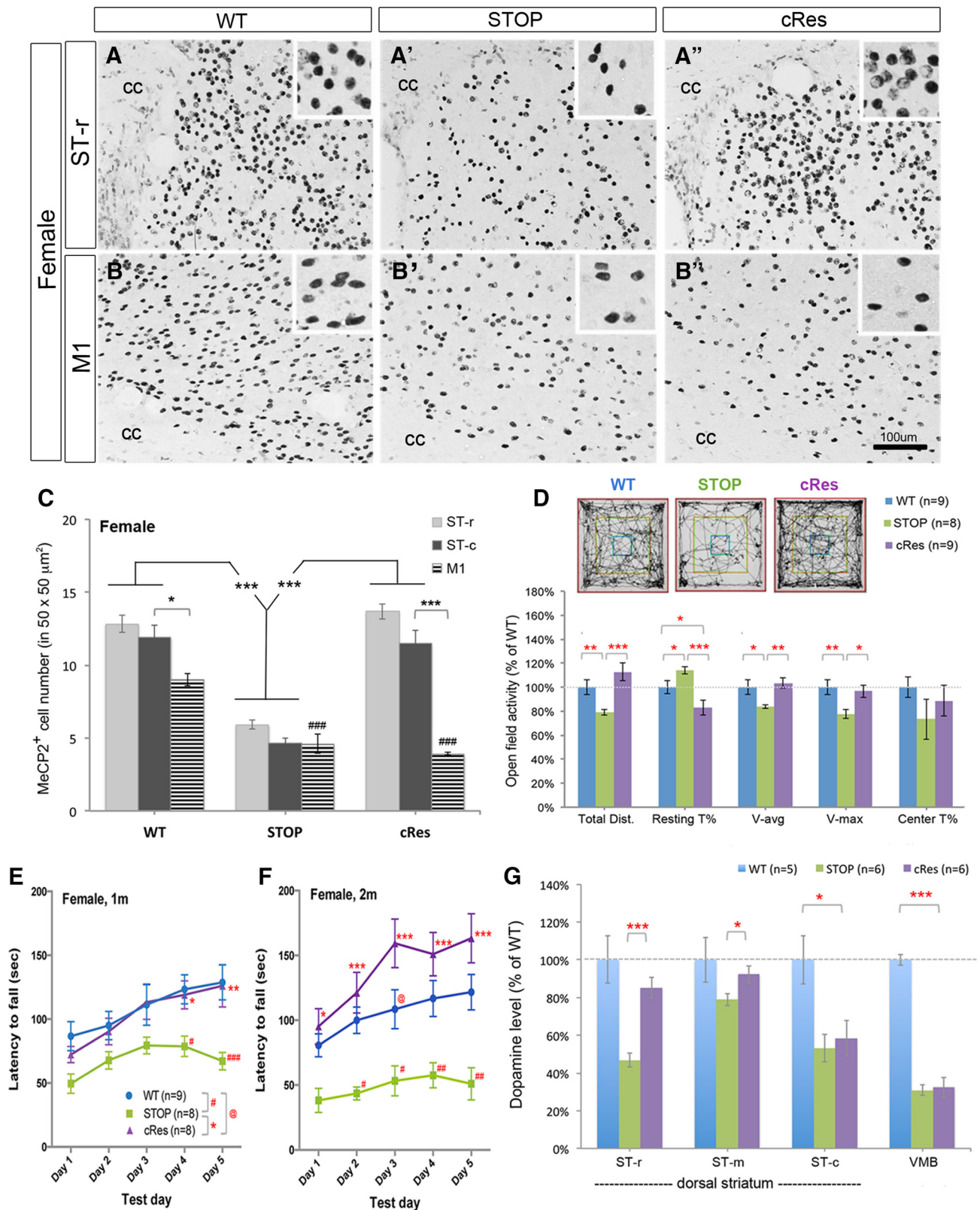
Figure 4. Expression of striatal MeCP2 preserves psychomotor function and dopamine content in female mice. *A–C*, Selective preservation of MeCP2 in the striatum of cRes female mice at 4–5 weeks of age. Insets show high-magnification images of MeCP2-positive nuclei in a square of $50 \times 50 \ \mu m^2$. Scale bar (in *B''*), 100 μm. cc, Corpus callosum. $n = 3$ for each group in *C*. *D*, Preserved locomotor activity in cRes female mice compared with WT and STOP females at 4–5 weeks of age. *E*, *F*, Complete restoration of motor skill learning in cRes female mice at 4–5 weeks of age (*E*). These cRes females performed even better than WT mice when retested at 8–10 weeks of age (*F*). *G*, Significant restoration of dopamine content in the ST-r and ST-m, but not in the ST-c and VMB of cRes mice. Data are shown as mean ± SEM; *, #, @$p < 0.05$; **, ##$p < 0.01$; ***, ###$p < 0.001$; compared with control mice (as indicated) by one-way ANOVA in *C*, *D*, and *G*; repeated measured two-way AVOVA in *E* and *F*, followed by Bonferroni *post hoc* test.
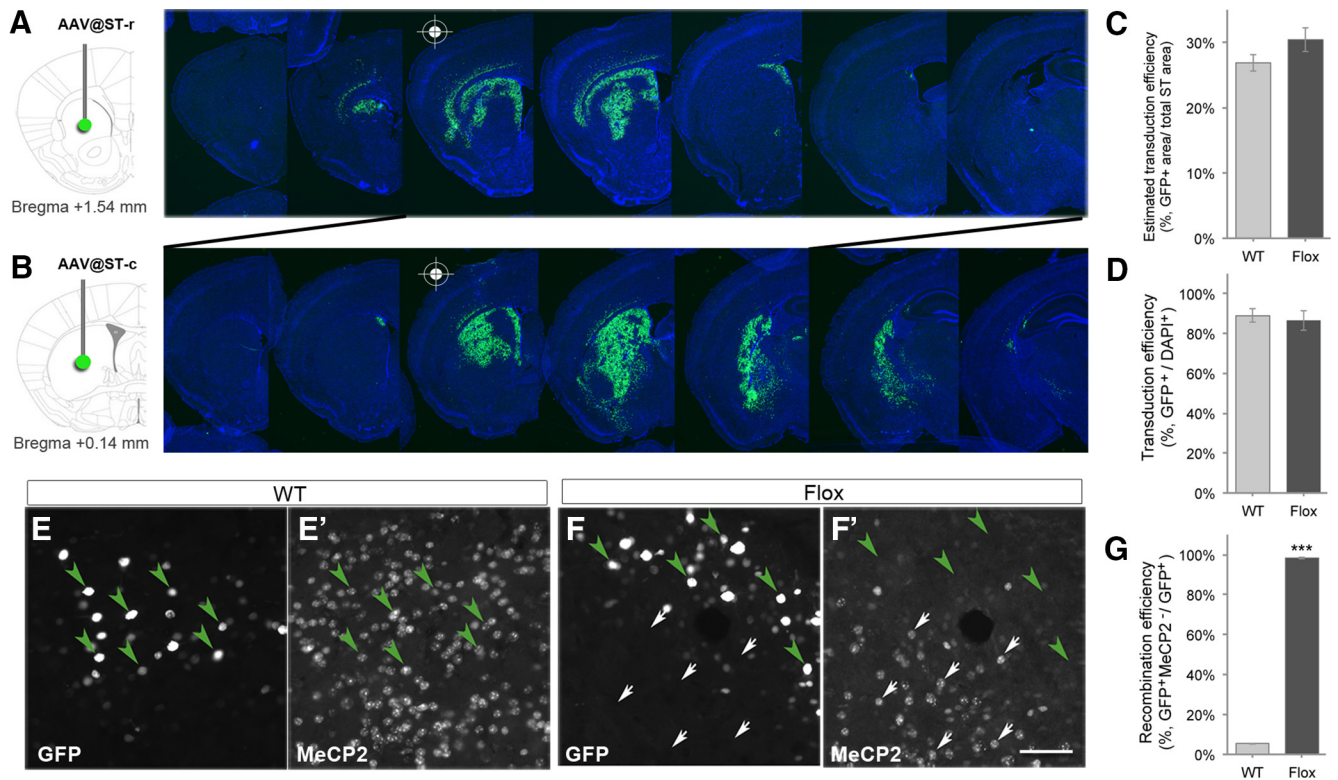
Figure 5. AAV-mediated focal deletion of *Mecp2* in the striatum. *A, B*, The Flox mice and their WT littermate controls at 4 –5 weeks of age were subjected to microinjection of AAV-Cre-GFP in the ST-r (*A*) or ST-c (*B*). Photomicrographs show GFP expression in the serial sections of AAV-treated brain counterstained by DAPI. *C, D*, Estimated transduction efficiency of AAV-Cre-GFP in the striatum. Similar transduction efficiency of AAV was found in Flox mice and WT controls. $n = 3$. *E–F′*, The GFP-positive cells in WT mice retain MeCP2 expression (*E, E′*, green arrowheads), whereas GFP-positive cells in Flox mice devoid of MeCP2 expression (*F, F′*, green arrowheads). Note that MeCP2 expression is remained in noninfected cells in Flox mice (*F, F′*, white arrows). *G*, The Cre-mediated recombination efficiency at the needle tip region is ~98% in Flox mice. Scale bar (in *F′*), 50 μm. ***$p < 0.001$, compared with WT by student t test.

$p < 0.001$) compared with saline-injected controls (Fig. 6H). The overelevated locomotor activities in Cre-positive STOP mice were similar to that in cRes male mice (Fig. 3E). Notably, the dopamine content was significantly lower in saline-treated STOP mice (35–57% of WT; Fig. 6I), but selectively restored to WT levels in the ST-r of AAV-treated STOP mice (108.3 ± 7.1% of WT, $p < 0.001$; Fig. 6I). Together, these findings demonstrate that MeCP2 plays a necessary and sufficient role in the striatum, especially in the ST-r, to maintain local dopamine content and modulate locomotor activity.

Discussion
Given the striking motor deficits and aberrant striatal features in mice lacking MeCP2 (Kao et al., 2015), we investigated the causality of striatal MeCP2 deficiency to the motor dysfunction of RTT. We found that loss of striatal MeCP2 reduced dopamine content and increased DRD2 expression in the ST-r, similar to that observed in *Mecp2*-null mice (Kao et al., 2015). Preservation of MeCP2 expression selectively in the striatum prevented hypoactivity and motor learning deficits in both male and female mice. Furthermore, spatially selective removal or preservation of MeCP2 expression in the ST-r significantly reduced or restored local dopamine content, and impaired or restored locomotion, respectively. These data suggest that MeCP2 in forebrain GABAergic neurons regulates dopamine content in the striatum in a subregion selective manner and that psychomotor function is particularly sensitive to MeCP2 function in the ST-r.

Previous studies demonstrated that impaired motor control in *Mecp2*-null mice is accompanied by decreased dopamine synthesis and structural/functional deficiencies in nigrostriatal do-

pamine neurons in the VMB (Gantz et al., 2011; Panayotis et al., 2011; Kao et al., 2015). Moreover, loss of MeCP2 in TH-positive aminergic neurons results in cell-autonomous reduction of dopamine synthesis and downregulation of TH expression (Samaco et al., 2009), suggesting that MeCP2 affects motor function by maintaining dopamine synthesis in midbrain dopaminergic neurons. In the present study, we found that ablation of striatal MeCP2 impaired locomotion and reduced dopamine content locally in the ST-r without affecting dopamine level in the VMB. In addition, reduced TH activity was found in the ST-r despite no change in total TH expression (Fig. 2D,E). These data suggest that MeCP2 in striatal GABAergic neurons influences dopaminergic afferents and modulates dopamine production in a non-cell autonomous manner. In addition, we found that DRD2 expression was significantly and selectively increased in the ST-r of cKO mice (Fig. 2E), similar to that observed in *Mecp2*-null mice (Kao et al., 2015) and RTT patients (Chiron et al., 1993). The increased DRD2 expression may either inhibit presynaptic TH activity (Lindgren et al., 2001) or reinforce the indirect pathway (Kreitzer and Malenka, 2008), thus leading to decreased dopamine synthesis and reduced motor activity. Mechanistically, our study does not exclude the possibility that other transcriptional targets of MeCP2, in addition to TH and DRD2, also play a role in this process. The retrograde signals originated from striatal neurons (Del-Bel et al., 2011; Sagi et al., 2014) may likely mediate MeCP2-dependent non-cell autonomous modulation of dopamine content in the striatum. In contrast to the ST-r, loss of striatal MeCP2 leads to an increase of TH expression and dopamine content in the ST-c, indicating a MeCP2-mediated non-cell
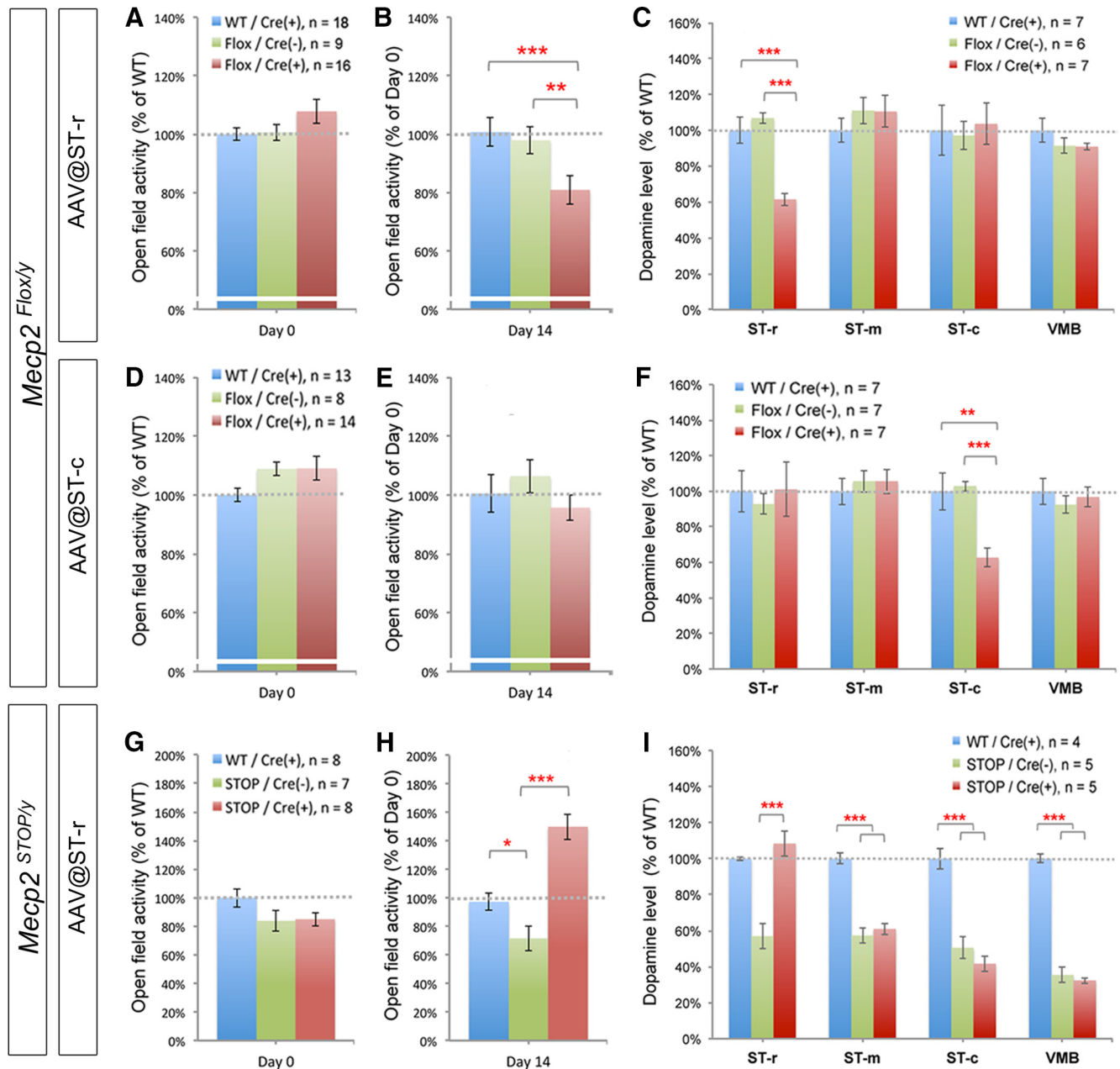
Figure 6. Region-specific ablation or reactivation of striatal MeCP2 alters local dopamine content and locomotor activity. **A–F**, Total distance traveled of mice at 4–5 weeks of age was measured in an open field before (**A**, **D**) or 14 d after (**B**, **E**) AAV injection, followed by dopamine measurement with HPLC (**C**, **F**). The Flox mice with AAV injection into ST-r [Flox/Cre (+)] traveled shorter distance (**B**) and contained lower dopamine content in the ST-r (**C**) compared with AAV-injected WT mice [WT/Cre(+)] and saline-injected Flox mice [Flox/Cre(−)]. Upon AAV injection to ST-c (**D–F**), Flox mice exhibit reduced local dopamine content in the ST-c (**F**) but normal open-field activity (**E**). **G–I**, Selective reactivation of MeCP2 in the ST-r of STOP mice restores both locomotor activity (**H**) and local dopamine content in the ST-r (**I**) 14 d after AAV injection. Locomotor activity of STOP mice before surgery (4–5 weeks old) was not significantly different from WT controls (**G**); *$p < 0.05$, **$p < 0.01$, ***$p < 0.001$, compared with indicated control mice by one-way AVOVA followed by Bonferroni *post hoc* test.

autonomous repression of TH expression in the caudal striatum. Given that MeCP2 has been reported to activate TH expression cell-autonomously in the VMB (Samaco et al., 2009), our data supports that MeCP2 likely plays distinct roles in the source and target areas of the nigrostriatal dopaminergic pathway.

The crucial role of striatal dopamine in psychomotor function has been well documented through the studies of Parkinson's disease (PD; Olanow et al., 2009). Our findings that: (1) the motor deficits-associated dopamine reduction was only detected in the ST-r, but not in the ST-m or ST-c of cKO mice, (2) preservation of dopamine content in the ST-r of cRes mice was accompanied by restored performance of locomotion and motor learning,

(3) focal deletion of *Mecp2* from the ST-r reduces dopamine content and impairs locomotion, and (4) focal preservation of *Mecp2* in the ST-r restores locomotion and local dopamine content of *Mecp2*-null mice, together suggest that MeCP2 selectively modulates regional dopamine content in the ST-r critical for motor outputs. Notably, previous studies have demonstrated that psychostimulant-induced reward behaviors require MeCP2 function in the nucleus accumbens, the ventral part of the ST-r (Deng et al., 2010, 2014), supporting the importance of MeCP2 at the ST-r in dopamine-related brain function. In contrast, we found that the dopamine level was increased in the ST-c in hypoactive cKO mice (Fig. 2C) and focal deletion of *Mecp2* in the ST-c

selectively reduced local dopamine content without affecting locomotor activity (Fig. 6*E,F*). These data suggest that dopamine content in the ST-c is not directly correlated to movement control.

The ST-r of rodents has long been considered equivalent to the caudate nucleus in primates that directly connects to the prefrontal cortex and orbitofrontal cortex (Graybiel, 2000) and has been implicated in motor learning, repetitive behavior, and cognitive functions, such as language and sociability (Crinion et al., 2006; Liao et al., 2008; Lawhorn et al., 2009; Kemp et al., 2013). Abnormal development or disrupted neurotransmission in the caudate nucleus has been observed in patients with autism, RTT, PD, and Huntington's disease (Blue et al., 1999; McAlonan et al., 2002; Langen et al., 2007; Niethammer et al., 2013; Padowski et al., 2014). In this study, we found that the dopamine content and DRD2 expression are selectively altered in the ST-r of *Mecp2*-cKO mice. Moreover, focal deletion or expression of MeCP2 in the ST-r is sufficient to disrupt or restore dopamine content and locomotor activity, respectively. Together, these data support that the ST-r is an anatomical origin for the psychomotor deficits of RTT. Given that RTT is likely a reversible condition (Guy et al., 2007) and an AAV-mediated gene therapy approach has found promising outcome in mouse models of RTT (Garg et al., 2013), our study suggests the caudate nucleus as a brain area for targeted therapeutics to ameliorate motor dysfunction in RTT.

References

Adachi M, Autry AE, Covington HE 3rd, Monteggia LM (2009) MeCP2-mediated transcription repression in the basolateral amygdala may underlie heightened anxiety in a mouse model of Rett syndrome. J Neurosci 29:4218–4227. CrossRef Medline

Amir RE, Van den Veyver IB, Wan M, Tran CQ, Francke U, Zoghbi HY (1999) Rett syndrome is caused by mutations in X-linked MECP2, encoding methyl-CpG-binding protein 2. Nat Genet 23:185–188. CrossRef Medline

Barnes CA (1979) Memory deficits associated with senescence: a neurophysiological and behavioral study in the rat. J Comp Physiol Psychol 93:74–104. CrossRef Medline

Blue ME, Naidu S, Johnston MV (1999) Altered development of glutamate and GABA receptors in the basal ganglia of girls with Rett syndrome. Exp Neurol 156:345–352. CrossRef Medline

Chahrour M, Zoghbi HY (2007) The story of Rett syndrome: from clinic to neurobiology. Neuron 56:422–437. CrossRef Medline

Chao HT, Chen H, Samaco RC, Xue M, Chahrour M, Yoo J, Neul JL, Gong S, Lu HC, Heintz N, Ekker M, Rubenstein JL, Noebels JL, Rosenmund C, Zoghbi HY (2010) Dysfunction in GABA signalling mediates autism-like stereotypies and Rett syndrome phenotypes. Nature 468:263–269. CrossRef Medline

Chen RZ, Akbarian S, Tudor M, Jaenisch R (2001) Deficiency of methyl-CpG binding protein-2 in CNS neurons results in a Rett-like phenotype in mice. Nat Genet 27:327–331. CrossRef Medline

Chiron C, Bulteau C, Loc'h C, Raynaud C, Garreau B, Syrota A, Mazière B (1993) Dopaminergic D2 receptor SPECT imaging in Rett syndrome: increase of specific binding in striatum. J Nucl Med 34:1717–1721. Medline

Cox MM, Tucker AM, Tang J, Talbot K, Richer DC, Yeh L, Arnold SE (2009) Neurobehavioral abnormalities in the dysbindin-1 mutant, sandy, on a C57BL/6J genetic background. Genes Brain Behav 8:390–397. CrossRef Medline

Crinion J, Turner R, Grogan A, Hanakawa T, Noppeney U, Devlin JT, Aso T, Urayama S, Fukuyama H, Stockton K, Usui K, Green DW, Price CJ (2006) Language control in the bilingual brain. Science 312:1537–1540. CrossRef Medline

Crittenden JR, Graybiel AM (2011) Basal ganglia disorders associated with imbalances in the striatal striosome and matrix compartments. Front Neuroanat 5:59. CrossRef Medline

Del-Bel E, Padovan-Neto FE, Raisman-Vozari R, Lazzarini M (2011) Role of nitric oxide in motor control: implications for Parkinson's disease pathophysiology and treatment. Curr Pharm Des 17:471–488. CrossRef Medline

Deng JV, Rodriguiz RM, Hutchinson AN, Kim IH, Wetsel WC, West AE (2010) MeCP2 in the nucleus accumbens contributes to neural and behavioral responses to psychostimulants. Nat Neurosci 13:1128–1136. CrossRef Medline

Deng JV, Wan Y, Wang X, Cohen S, Wetsel WC, Greenberg ME, Kenny PJ, Calakos N, West AE (2014) MeCP2 phosphorylation limits psychostimulant-induced behavioral and neuronal plasticity. J Neurosci 34:4519–4527. CrossRef Medline

Funakoshi H, Okuno S, Fujisawa H (1991) Different effects on activity caused by phosphorylation of tyrosine hydroxylase at serine 40 by three multifunctional protein kinases. J Biol Chem 266:15614–15620. Medline

Gantz SC, Ford CP, Neve KA, Williams JT (2011) Loss of Mecp2 in substantia nigra dopamine neurons compromises the nigrostriatal pathway. J Neurosci 31:12629–12637. CrossRef Medline

Garg SK, Lioy DT, Cheval H, McGann JC, Bissonnette JM, Murtha MJ, Foust KD, Kaspar BK, Bird A, Mandel G (2013) Systemic delivery of MeCP2 rescues behavioral and cellular deficits in female mouse models of Rett syndrome. J Neurosci 33:13612–13620. CrossRef Medline

Goffin D, Allen M, Zhang L, Amorim M, Wang IT, Reyes AR, Mercado-Berton A, Ong C, Cohen S, Hu L, Blendy JA, Carlson GC, Siegel SJ, Greenberg ME, Zhou Z (2012) Rett syndrome mutation MeCP2 T158A disrupts DNA binding, protein stability and ERP responses. Nat Neurosci 15:274–283. CrossRef Medline

Goffin D, Brodkin ES, Blendy JA, Siegel SJ, Zhou Z (2014) Cellular origins of auditory event-related potential deficits in Rett syndrome. Nat Neurosci 17:804–806. CrossRef Medline

Graybiel AM (2000) The basal ganglia. Curr Biol 10:R509–R511. CrossRef Medline

Guy J, Hendrich B, Holmes M, Martin JE, Bird A (2001) A mouse Mecp2-null mutation causes neurological symptoms that mimic Rett syndrome. Nat Genet 27:322–326. CrossRef Medline

Guy J, Gan J, Selfridge J, Cobb S, Bird A (2007) Reversal of neurological defects in a mouse model of Rett syndrome. Science 315:1143–1147. CrossRef Medline

Guy J, Cheval H, Selfridge J, Bird A (2011) The role of MeCP2 in the brain. Annu Rev Cell Dev Biol 27:631–652. CrossRef Medline

Kao FC, Su SH, Carlson GC, Liao W (2015) MeCP2-mediated alterations of striatal features accompany psychomotor deficits in a mouse model of Rett syndrome. Brain Struct Funct 220:419–434. CrossRef Medline

Kemp J, Berthel MC, Dufour A, Després O, Henry A, Namer IJ, Musacchio M, Sellal F (2013) Caudate nucleus and social cognition: neuropsychological and SPECT evidence from a patient with focal caudate lesion. Cortex 49:559–571. CrossRef Medline

Kreitzer AC, Malenka RC (2008) Striatal plasticity and basal ganglia circuit function. Neuron 60:543–554. CrossRef Medline

Lang M, Wither RG, Brotchie JM, Wu C, Zhang L, Eubanks JH (2013) Selective preservation of MeCP2 in catecholaminergic cells is sufficient to improve the behavioral phenotype of male and female Mecp2-deficient mice. Hum Mol Genet 22:358–371. CrossRef Medline

Langen M, Durston S, Staal WG, Palmen SJ, van Engeland H (2007) Caudate nucleus is enlarged in high-functioning medication-naive subjects with autism. Biol Psychiatry 62:262–266. CrossRef Medline

Lawhorn C, Smith DM, Brown LL (2009) Partial ablation of mu-opioid receptor rich striosomes produces deficits on a motor-skill learning task. Neuroscience 163:109–119. CrossRef Medline

Liao WL, Wang HF, Tsai HC, Chambon P, Wagner M, Kakizuka A, Liu FC (2005) Retinoid signaling competence and RARbeta-mediated gene regulation in the developing mammalian telencephalon. Dev Dyn 232:887–900. CrossRef Medline

Liao WL, Tsai HC, Wang HF, Chang J, Lu KM, Wu HL, Lee YC, Tsai TF, Takahashi H, Wagner M, Ghyselinck NB, Chambon P, Liu FC (2008) Modular patterning of structure and function of the striatum by retinoid receptor signaling. Proc Natl Acad Sci U S A 105:6765–6770. CrossRef Medline

Lindgren N, Xu ZQ, Herrera-Marschitz M, Haycock J, Hökfelt T, Fisone G (2001) Dopamine D(2) receptors regulate tyrosine hydroxylase activity and phosphorylation at Ser40 in rat striatum. Eur J Neurosci 13:773–780. CrossRef Medline

McAlonan GM, Daly E, Kumari V, Critchley HD, van Amelsvoort T, Suckling J, Simmons A, Sigmundsson T, Greenwood K, Russell A, Schmitz N, Happe F, Howlin P, Murphy DG (2002) Brain anatomy and sensorimo-

tor gating in Asperger's syndrome. Brain 125:1594–1606. CrossRef Medline

Monory K, Massa F, Egertová M, Eder M, Blaudzun H, Westenbroek R, Kelsch W, Jacob W, Marsch R, Ekker M, Long J, Rubenstein JL, Goebbels S, Nave KA, During M, Klugmann M, Wölfel B, Dodt HU, Zieglgänsberger W, Wotjak CT, et al. (2006) The endocannabinoid system controls key epileptogenic circuits in the hippocampus. Neuron 51:455–466. CrossRef Medline

Niethammer M, Tang CC, Ma Y, Mattis PJ, Ko JH, Dhawan V, Eidelberg D (2013) Parkinson's disease cognitive network correlates with caudate dopamine. Neuroimage 78:204–209. CrossRef Medline

Ohtsuka N, Tansky MF, Kuang H, Kourrich S, Thomas MJ, Rubenstein JL, Ekker M, Leeman SE, Tsien JZ (2008) Functional disturbances in the striatum by region-specific ablation of NMDA receptors. Proc Natl Acad Sci U S A 105:12961–12966. CrossRef Medline

Olanow CW, Kordower JH, Lang AE, Obeso JA (2009) Dopaminergic transplantation for Parkinson's disease: current status and future prospects. Ann Neurol 66:591–596. CrossRef Medline

Padowski JM, Weaver KE, Richards TL, Laurino MY, Samii A, Aylward EH, Conley KE (2014) Neurochemical correlates of caudate atrophy in Huntington's disease. Mov Disord 29:327–335. CrossRef Medline

Panayotis N, Pratte M, Borges-Correia A, Ghata A, Villard L, Roux JC (2011) Morphological and functional alterations in the substantia nigra pars compacta of the Mecp2-null mouse. Neurobiol Dis 41:385–397. CrossRef Medline

Paxinos G, Franklin KBJ (2004) The mouse brain in stereotaxic coordinates. Amsterdam: Elsvier.

Peça J, Feliciano C, Ting JT, Wang W, Wells MF, Venkatraman TN, Lascola CD, Fu Z, Feng G (2011) Shank3 mutant mice display autistic-like behaviours and striatal dysfunction. Nature 472:437–442. CrossRef Medline

Sagi Y, Heiman M, Peterson JD, Musatov S, Kaplitt MG, Surmeier DJ, Heintz N, Greengard P (2014) Nitric oxide regulates synaptic transmission between spiny projection neurons. Proc Natl Acad Sci U S A 111:17636–17641. CrossRef Medline

Samaco RC, Mandel-Brehm C, Chao HT, Ward CS, Fyffe-Maricich SL, Ren J,

Hyland K, Thaller C, Maricich SM, Humphreys P, Greer JJ, Percy A, Glaze DG, Zoghbi HY, Neul JL (2009) Loss of MeCP2 in aminergic neurons causes cell-autonomous defects in neurotransmitter synthesis and specific behavioral abnormalities. Proc Natl Acad Sci U S A 106:21966–21971. CrossRef Medline

Shahbazian M, Young J, Yuva-Paylor L, Spencer C, Antalffy B, Noebels J, Armstrong D, Paylor R, Zoghbi H (2002) Mice with truncated MeCP2 recapitulate many Rett syndrome features and display hyperacetylation of histone H3. Neuron 35:243–254. CrossRef Medline

Shen HY, Coelho JE, Ohtsuka N, Canas PM, Day YJ, Huang QY, Rebola N, Yu L, Boison D, Cunha RA, Linden J, Tsien JZ, Chen JF (2008) A critical role of the adenosine A2A receptor in extrastriatal neurons in modulating psychomotor activity as revealed by opposite phenotypes of striatum and forebrain A2A receptor knock-outs. J Neurosci 28:2970–2975. CrossRef Medline

Shepherd JK, Grewal SS, Fletcher A, Bill DJ, Dourish CT (1994) Behavioural and pharmacological characterisation of the elevated "zero-maze" as an animal model of anxiety. Psychopharmacology (Berl) 116:56–64. CrossRef Medline

Temudo T, Ramos E, Dias K, Barbot C, Vieira JP, Moreira A, Calado E, Carrilho I, Oliveira G, Levy A, Fonseca M, Cabral A, Cabral P, Monteiro JP, Borges L, Gomes R, Santos M, Sequeiros J, Maciel P (2008) Movement disorders in Rett syndrome: an analysis of 60 patients with detected MECP2 mutation and correlation with mutation type. Mov Disord 23:1384–1390. CrossRef Medline

Yu C, Gupta J, Chen JF, Yin HH (2009) Genetic deletion of A2A adenosine receptors in the striatum selectively impairs habit formation. J Neurosci 29:15100–15103. CrossRef Medline

Zhao YT, Goffin D, Johnson BS, Zhou Z (2013) Loss of MeCP2 function is associated with distinct gene expression changes in the striatum. Neurobiol Dis 59:257–266. CrossRef Medline

Zhou Z, Hong EJ, Cohen S, Zhao WN, Ho HY, Schmidt L, Chen WG, Lin Y, Savner E, Griffith EC, Hu L, Steen JA, Weitz CJ, Greenberg ME (2006) Brain-specific phosphorylation of MeCP2 regulates activity-dependent Bdnf transcription, dendritic growth, and spine maturation. Neuron 52:255–269. CrossRef Medline